Geochemistry Geophysics Geosystems G3

Article
Volume 11, Number 11
10 November 2010
Q11006, doi:10.1029/2010GC003276
ISSN: 1525-2027

Published by AGU and the Geochemical Society

Development of the Australian-Antarctic depth anomaly

Joanne M. Whittaker and R. Dietmar Müller
EarthByte Group, School of Geosciences, University of Sydney, Sydney, New South Wales 2006, Australia (jo.whittaker@sydney.edu.au)

Michael Gurnis
Seismological Laboratory, California Institute of Technology, Pasadena, California 91125, USA

[1] The oceanic Australian-Antarctic Discordance (AAD) contains two unusual features: (1) N–S trending anomalously deep bathymetries and (2) rough basement morphologies in young (<~20 Ma) crust between 120°E and 128°E. Models generally attribute AAD formation to underlying cold and/or depleted upper mantle, but no model adequately accounts for all the anomalous attributes. We quantify anomalous basement roughness and basement depths utilizing new seismic reflection data, in combination with all available geophysical and geological observations. We find that the interaction of negative dynamic topography and crustal thickness variations results in the observed complex patterns of residual basement depths. Downwelling, caused by a sinking Mesozoic slab, is the most likely cause of the broad N–S trending residual depth anomalies, while overprinting by westward flowing, buoyant Pacific mantle resulted in the distinctive V-shaped eastern boundary of the AAD. The particularly large residual depths proximal to the Australian and Antarctic margins may be due to negative dynamic topography combined with thinned oceanic crust caused by ultraslow (<10 mm/yr) half-spreading rates and sampling of depleted subduction wedge contaminated mantle. Only oceanic basement aged <20 Ma is anomalously rough, a result of sampling of cool/depleted upper mantle material. Although oceanic crust older than 43 Ma may have sampled depleted mantle, the resulting oceanic basement is not anomalously rough likely because a melt volume controlled threshold of accretion-related roughness had already been reached due to ultraslow spreading rates. Our analysis reveals that the enigmatic roughness of the Diamantina Zone is mainly related to >45° spreading obliquities.

Components: 10,500 words, 10 figures.

Keywords: oceanic accretion; mantle dynamics.

Index Terms: 3045 Marine Geology and Geophysics: Seafloor morphology, geology, and geophysics; 3035 Marine Geology and Geophysics: Midocean ridge processes; 3010 Marine Geology and Geophysics: Gravity and isostasy (1218, 1222).

Received 12 July 2010; **Revised** 9 September 2010; **Accepted** 14 September 2010; **Published** 10 November 2010.

Whittaker, J. M., R. D. Müller, and M. Gurnis (2010), Development of the Australian-Antarctic depth anomaly, *Geochem. Geophys. Geosyst.*, *11*, Q11006, doi:10.1029/2010GC003276.

1. Introduction

[2] The Southern Ocean between Australia and Antarctica encompasses a large swath of anomalously deep oceanic basement, which defines the extent of the AAD. The best way to view the extent of this unusual bathymetry is through maps of residual depth anomaly where normal ocean-lithospheric subsidence and sediment loading are removed from observed bathymetry [e.g., *Crough*, 1983]. In the

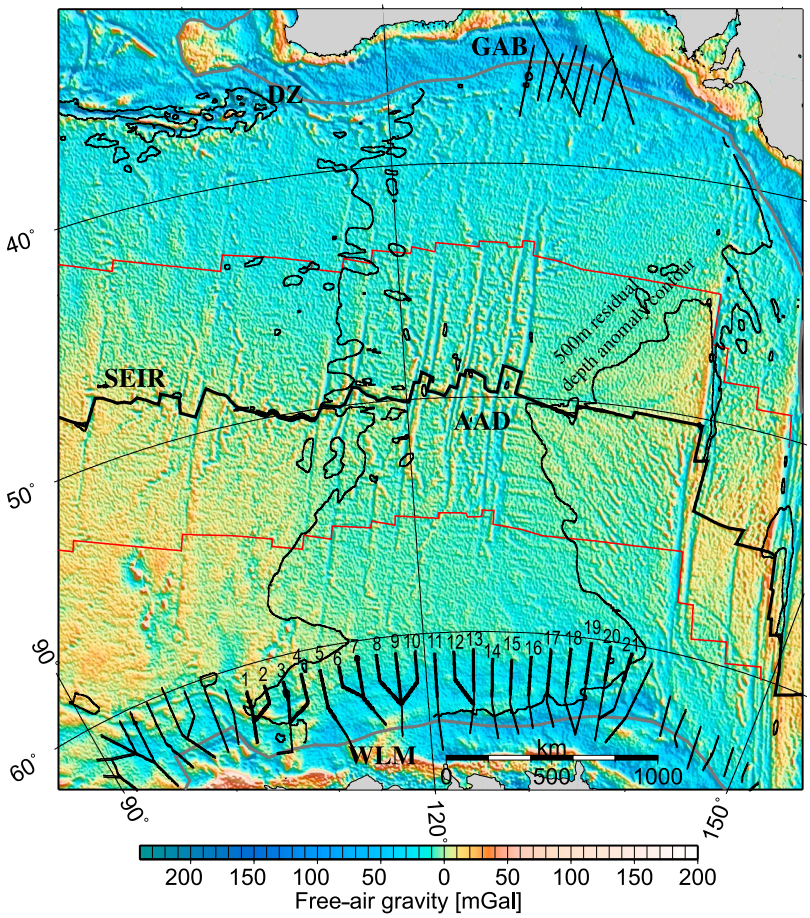

Figure 1. Regional 1 min marine gravity anomaly map [*Sandwell and Smith*, 2005] illustrating the main structural elements of the southeast Indian Ocean using an illumination azimuth of 45°. Overlain are deep seismic profile locations (black lines) along the Australian and Antarctic margins, the location of the Southeast Indian Ridge, and a revised estimate of the location of the 500 m RDA contour. Also shown is the rough basement morphology of the Australian-Antarctic Discordance (AAD), Great Australian Bight (GAB), Southeast Indian Ridge (SEIR), Diamantina Zone (DZ), and Wilkes Land Margin (WLM). The projection is a Lambert equal area projection, with a center at 125°E and 50°S. Red lines are the 20 Ma isochron on each flank of the Southeast Indian Ridge. Thin black lines show locations of ship tracks, and bold sections represent the locations of profiles shown in Figure 7.

Southern Ocean, the resulting depth anomaly encompasses a broad N–S trending band of oceanic crust (Figure 1). *Hayes and Conolly* [1972] first mapped the anomalous depths of the Southeast Indian Ridge between the longitudes of 120°E and 128°E. Using maps of residual depth, *Marks et al.* [1990] found the depth anomaly extended north and south from the Southeast Indian Ridge in an arcuate, symmetrical pattern. *Gurnis and Müller* [2003] used the same technique to show that the residual depth anomaly extends from the Southeast Indian Ridge to the Australian and Antarctic margins with an hourglass geometry where the depth anomaly becomes wider and deeper toward the passive margins. There is also evidence that the anomalous depths may continue onshore Australia and Antarctica [*Veevers*, 1982]. This feature, defined by tracing the relative highs running roughly from north to south at its flanks, has been linked to Australian and Antarctica topographic features as old as the Carboniferous [*Veevers*, 1982] and the Cretaceous marine inundation of Australia which was out of phase with global sea level variations [*Gurnis et al.*, 1998].

[3] The oceanic crust between Australia and Antarctica also exhibits other unusual morphologic characteristics. Within the AAD is a region of young (<~20 Ma) oceanic crust characterized by distinctive basement morphologies, with closely spaced fracture zones and irregular basement blocks characterized by high-amplitude topographic relief of 600–1000 m, at ~15 km wavelength [*Weissel and Hayes*, 1971] and a lack of axis-parallel fab-

rics typical of abyssal plains [*Christie et al.*, 1998]. This distinctive oceanic basement occurs between ~120°E and ~128°E, straddling the deepest (4–5 km) section of the global mid-ocean ridge system (Figure 1). The AAD is one of the most highly segmented sections of the Southeast Indian Ridge with a complex pattern of short, deep axial valleys that are offset by left and right stepping fracture zones [e.g., *Christie et al.*, 2004; *Marks et al.*, 1999; *Small et al.*, 1999].

[4] In addition to uncommonly deep bathymetries and distinctive basement morphologies, a number of other unusual geological characteristics occur in the AAD. Wide-angle seismic refraction reveals that crust proximal to the ridge within the AAD is only 3.6–4.2 km thick, considerably thinner than 7–7.5 km thick oceanic crust found to the east, and 7.2 km thick crust to the west [*Holmes et al.*, 2010].

[5] Geochemical analyses of dredged basalts reveal that the boundary between Pacific MORB source mantle (Pacific mantle) and Indian MORB source mantle (Indian mantle) lies close to the eastern boundary of the AAD [*Christie et al.*, 1998; *Pyle et al.*, 1995]. The close association between the residual depth anomaly and the Indian-Pacific mantle boundary has existed since ~28 Ma [*Christie et al.*, 2004; *Marks et al.*, 1990].

[6] A clear understanding of the anomalous features within the AAD is crucial to unraveling the mechanism(s) responsible for forming these features. A long-standing problem concerns a poor understanding of the spatial extent of the distinctive AAD basement morphologies. *Christie et al.* [1998] argued that "chaotic" basement extended to crust formed at least 30 Ma based on swath bathymetry, while *Marks et al.* [1999] found that the onset of the unusual basement morphologies was at approximately 20 Ma.

[7] Almost all models [e.g., *Forsyth et al.*, 1987; *Hayes*, 1988; *Klein et al.*, 1988; *Kuo*, 1993; *Kuo et al.*, 1996; *West et al.*, 1997] have assumed that the rough basement morphologies and residual depth anomaly of the AAD are spatially correlated and formed by the same process(es). However, recently, the eastern boundaries of the rough basement and residual depth anomaly have been found to be geographically distinct, having come into alignment only since ~12 Ma [*Christie et al.*, 2004]. *Gurnis and Müller* [2003] also noted the independent nature of these features, observing that rough basement morphologies are restricted to oceanic basement <~20–30 Ma, while the residual depth anomaly extended to the continental margins and also, possibly onshore.

[8] Most early models focused on the young (<20–30 Ma) portion of the AAD and sought mechanisms that explained the formation of both the rough ocean basement and the residual depth anomaly. One group of models invoked downwelling mantle material beneath the Southeast Indian Ridge as the main mechanism responsible for forming the AAD [e.g., *Hayes*, 1988; *Klein et al.*, 1988]. However, this proposal implies the paradoxical presence of downwelling mantle within a mid-ocean ridge system that is normally associated with upwelling. Later models attempted to avoid this geodynamic problem by proposing that the anomalous depths and basement morphologies were related to inhibited mantle upwelling [*Kuo*, 1993; *Kuo et al.*, 1996] or that downwelling was related to passive westward mantle flow along the axis of the Southeast Indian Ridge from the Pacific toward cold upper mantle located beneath the AAD [*Forsyth et al.*, 1987; *West et al.*, 1997]. The presence of cool mantle material beneath the AAD has long been proposed. *Weissel and Hayes* [1974] and *Hayes* [1976] proposed a stable, suspended mantle cold spot that migrated with the Southeast Indian Ridge, although how the cold spot remained beneath the Southeast Indian Ridge is geodynamically problematic. *Lin et al.* [2002] suggested that ascending cold material beneath the mid-ocean ridge can only be sustained for ~20–40 Ma following continental rifting.

[9] Recently, *Buck et al.* [2009] proposed a variant mantle flow model for the formation of the AAD. In this hypothesis the deep roots of Australia and Antarctica inhibited upper mantle replenishment as they separated, eventually leading to the development of thin and depleted asthenosphere beneath the AAD portion of the Southeast Indian Ridge [*Buck et al.*, 2009]. Similarly to many earlier hypotheses this model assumes that the depth anomaly and the anomalous basement were formed by the same mechanism and does not attempt to account for the changing basement morphologies perpendicular to the ridge. Also, the AAD is a globally unique feature and deep continental roots that separate following continental breakup are not, making it unclear as to why AAD-type features are not found in more ocean basins formed during the breakup of Pangaea.

[10] A third, alternative model for the formation of the AAD utilizes a westward dipping Mesozoic subducted slab [*Gurnis et al.*, 1998, 2000]. This hypothesis has two components. First, down-

welling ancient slab material trending roughly N–S at depth is responsible for the depth anomaly. Second, cool/depleted slab material has been progressively drawn up beneath the mid-ocean ridge following continental breakup and was first sampled at the mid-ocean ridge at 20 Ma, some 25 million years after the onset of fast spreading between Australia and Antarctica at ~45 Ma. A fast seismic velocity structure imaged in the upper mantle beneath the AAD support a subducted slab origin [*Ritzwoller et al.*, 2003]. The upper mantle anomaly is tomographically imaged as striking NW–SE [*Ritzwoller et al.*, 2003], but geodynamically modeled as N–S trending [*Gurnis et al.*, 1998]. This discrepancy is most likely due to the poorly constrained Mesozoic subduction zone geometry, uncertainties in mantle tomographic images, or a combination of both.

[11] While the formation of the rough <20 Myr old crust of the AAD has been addressed extensively, only one model [*Gurnis and Müller*, 2003] has attempted to explain the formation of anomalous crust across the entire Australian Southern Ocean. Two crucial observations need to be accounted for: (1) the depth anomaly is most prominent (broadest and deepest) proximal to the Australian and Antarctic continental margins and (2) the ocean basement morphology changes across the AAD. *Gurnis and Müller* [2003] expanded on their previous model and proposed that, following cessation of Mesozoic subduction, ancient mantle wedge material remained in the upper mantle. Following the onset of seafloor spreading at ~83 Ma this anomalous mantle was immediately sampled by the Southeast Indian Ridge leading to the formation of the large depth anomalies observed close to both margins.

[12] In essence, the *Gurnis and Müller* [2003] model proposes a link between the deep mantle and the upper mantle in order to explain both the residual depth anomaly and the changing morphologies of the oceanic crust across the Southern Ocean. This model proposed a downwelling slab (cool mantle) at depth to explain the residual depth anomaly combined with three stages of oceanic crustal accretion. Ocean crust proximal to the Australian and Antarctic continental margins formed as the Southeast Indian Ridge sampled depleted upper mantle derived from an ancient wedge. The young (<25 Ma), rough ocean basement of the AAD formed from cool and/or depleted upper mantle derived from the ancient downwelling slab. Oceanic crust formed in between these two end-members can be assumed to have sampled "normal" upper mantle material. Cool/depleted mantle material is believed to result in the accretion of oceanic basement exhibiting rougher oceanic basement morphologies [*Meyzen et al.*, 2003]. An implication of the *Gurnis and Müller* [2003] model is that both the youngest AAD oceanic basement and the oldest, margin proximal oceanic basement should exhibit basement morphologies that are much rougher than average oceanic basement. An additional issue is that the distinctive V shape of the eastern boundary of the residual depth anomaly is not adequately explained.

2. Methods

[13] We employ recent, high-resolution global satellite-derived gravity, and sediment thickness estimates derived from recently acquired seismic reflection data, to compute the shape, extent and magnitude of the depth anomalies and the anomalous basement roughness of the AAD.

2.1. Basement Roughness

[14] In order to analyze the oceanic basement of the Southern Ocean we apply the methodology of *Whittaker et al.* [2008] to compute a roughness grid. Oceanic basement roughness varies globally and relationships between roughness, sediment thickness, seafloor spreading rates, and spreading obliquities have been quantified. For four regions, Broken Ridge-Kerguelen Plateau (BRKP), West AAD, AAD, and East AAD (see Figure 2), we compute expected basement roughness given spreading rate (Figure 3b) and sediment thickness (Figure 4b). In order to determine areas of oceanic crust that exhibit anomalously rough or smooth ocean basement we compare our observed roughness against computed roughness for each area in 5 Ma bins of ocean crust (Figure 5). Computation of residual roughness removes roughness variations attributed to spreading rate, sediment thickness and spreading obliquity. Remaining patterns of residual roughness are likely attributable to variations in mantle temperature and magmatic fertility [*Whittaker et al.*, 2008], or possibly to other unknown parameters.

[15] Our analysis of roughness includes roughness attributable to both fracture zones and abyssal plains. It should be noted that where we use the term "chaotic" in reference to basement morphologies, we use in the context of *Christie et al.* [1998] to refer only to the fabric of the oceanic crust between fracture zones, but excluding the fracture zones themselves.

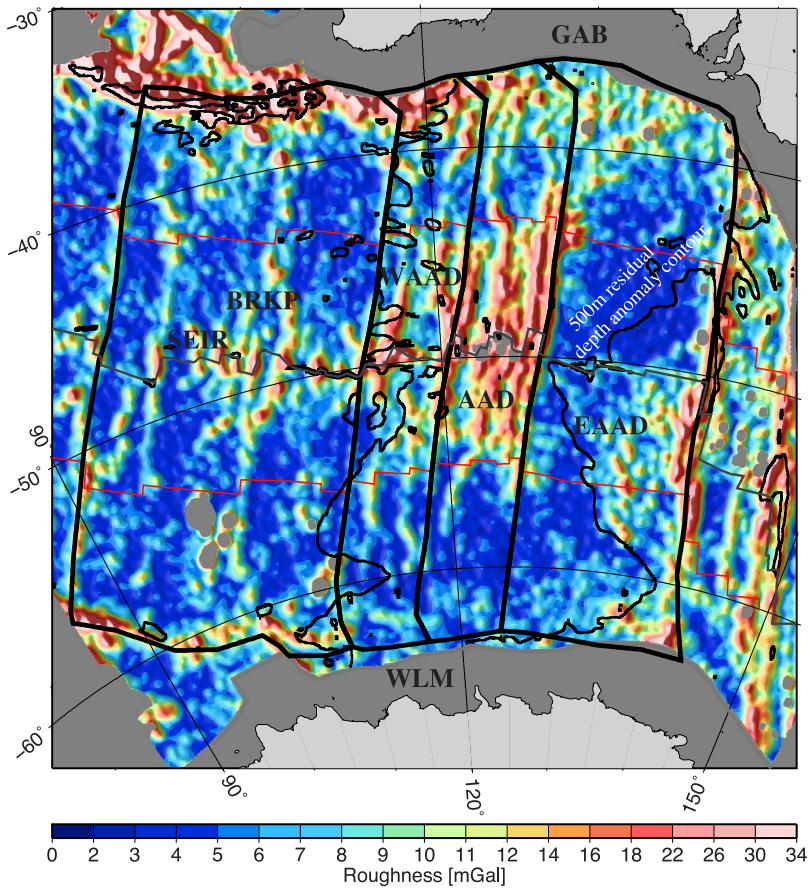

Figure 2. Downward continued gravity RMS roughness calculated using a Gaussian filter with a half-width of 50 km. Four analysis regions are outlined in thick black lines: Broken Ridge Kerguelen Plateau (BRKP), West AAD (WAAD), AAD, and East AAD (EAAD). Red lines are the 20 Ma isochron on each flank of the Southeast Indian Ridge.

[16] The longitudinal boundaries of the four regions in our analysis follow tectonic flowlines seeded at the Southeast Indian Ridge at 120°E and 128°E, for the eastern and western boundaries of the AAD. The western boundary of WAAD was seeded at the fracture zone at ~115E, marking the western extent of rough basement evident in satellite gravity (Figure 1). Further west, the BRKP region does not exhibit either rough basement morphologies or a residual depth anomaly, and so provides a good comparison for the AAD with oceanic crust resulting from typical Indian-type mantle.

2.2. Residual Depth Anomaly

[17] Previously, computation of the AAD residual depth anomaly, has revealed the anomaly becomes wider and deeper toward both the passive continental margins, e.g., hourglass in shape [*Gurnis and Müller*, 2003]. However, previously the sediment thickness maps used were poorly constrained, even though the sediment correction on the Antarctic margin was large.

[18] To improve the accuracy of the residual depth anomaly we incorporate new sediment thickness information obtained from seismic reflection data from the Australian and Antarctic margins (Figures 6 and 7). During the Antarctic summers of 2000/01 and 2001/02, Geoscience Australia acquired a major deep water geophysical data set off the East Antarctica margin (~36°E–152°E), which included high-quality deeply penetrating multichannel seismic data with coincident gravity, magnetic and bathymetry [*Stagg and Colwell*, 2003]. Interpretation of sediment thickness and depth to igneous basement along profiles off the Wilkes Land margin (Figures 6 and 7) provide observations that we have used to improve the residual depth anomaly map on Cretaceous aged crust. The regional high-resolution sediment

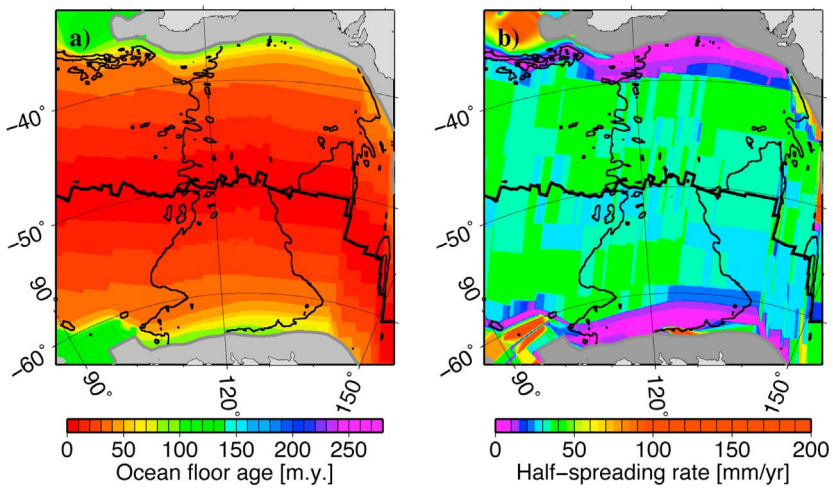

Figure 3. (a) Regional map showing color-coded oceanic age using the following isochrons, using the *Cande and Kent* [1995] and *Gradstein et al.* [1994] time scales from young to old: C5 (10.9 Ma), C6 (20.1 Ma), C13 (33.1 Ma), C18 (40.1 Ma), C21 (47.9 Ma), C25 (55.9 Ma), C31 (67.7 Ma) C34 (83.5 Ma), 100 Ma, M0 (120.4 Ma), and M4 (131.9 Ma). (b) Regional map showing spreading half rates The 500 m depth anomaly is plotted as a thin black line, and the bold black line shows the current location of the Southeast Indian Ridge. Regions of continental crust are shaded in gray.

thickness grid for the Wilkes Land was merged with sediment thickness data from *Géli et al.* [2007] and the NGDC global sediment thickness grid [*Divins*, 2004] to create a sediment thickness grid for the Australian Southern Ocean with substantially improved sediment thicknesses for the margins as well the AAD region (Figure 4b).

[19] To calculate the residual depth anomaly grid (RDA) (Figures 4d and 8), where the effects of sediment loading and crustal age have been removed, we start with a predicted bathymetry grid (ETOPO2v2). To compute unloaded igneous basement (IB_U) depth (Figure 4c) we correct for sediment loading using predicted bathymetry [*Smith and Sandwell*, 1997], sediment thicknesses (Figure 4b) and the procedure outlined by *Sykes* [1996]. The residual depth anomaly grid, *RDA*, is then created by removing the unloaded basement grid (IB_U) (Figure 4c) from the grid of predicted depth to igneous basement (IB_P) (Figure 4a), which estimates the average depth of comparably aged oceanic crust. The predicted depth to igneous basement (IB_P) is calculated using the seafloor age grid from *Müller et al.* [2008] and the *Pribac* [1991] thermal boundary layer model that describes the relationship between the depth of the seafloor and its age. The *Pribac* [1991] age-depth was selected because it accounts for conductive cooling of the oceanic lithosphere between a deeper than normal ridge crest and its flanks (ridge crest depth = 2600 m, subsidence constant = 220 m/m.y.$^{1/2}$).

$$IB_P = -2600 - 220\sqrt{t}, \text{ where t is time in million years.} \quad (1)$$

$$RDA = IB_P - IB_U \quad (2)$$

[20] Residual depth anomalies in oceanic crust are caused by two main mechanisms, crustal thickness variations and dynamic topography. In order to investigate whether crustal thickness anomalies alone are sufficient to explain the residual depth patterns in the AAD we compute an oceanic crustal thickness grid (Figure 10). We estimate oceanic crustal thickness based on the assumption that the entire depth anomaly is due to crustal thickness variations, following the method of *Louden et al.* [2004] assuming the average oceanic crustal density of 2.95 Mg/m3, water density of 1.03 Mg/m3, mantle density of 3.3 Mg/m3 and average oceanic crustal thickness of 7 km [*White et al.*, 1992].

3. Results

[21] The free-air gravity (Figure 1) and RMS roughness (Figure 2) show that basement morphologies are highly variable in the Australian Southern Ocean. Within the AAD and WAAD, rough basement extends across both flanks of the Southeast

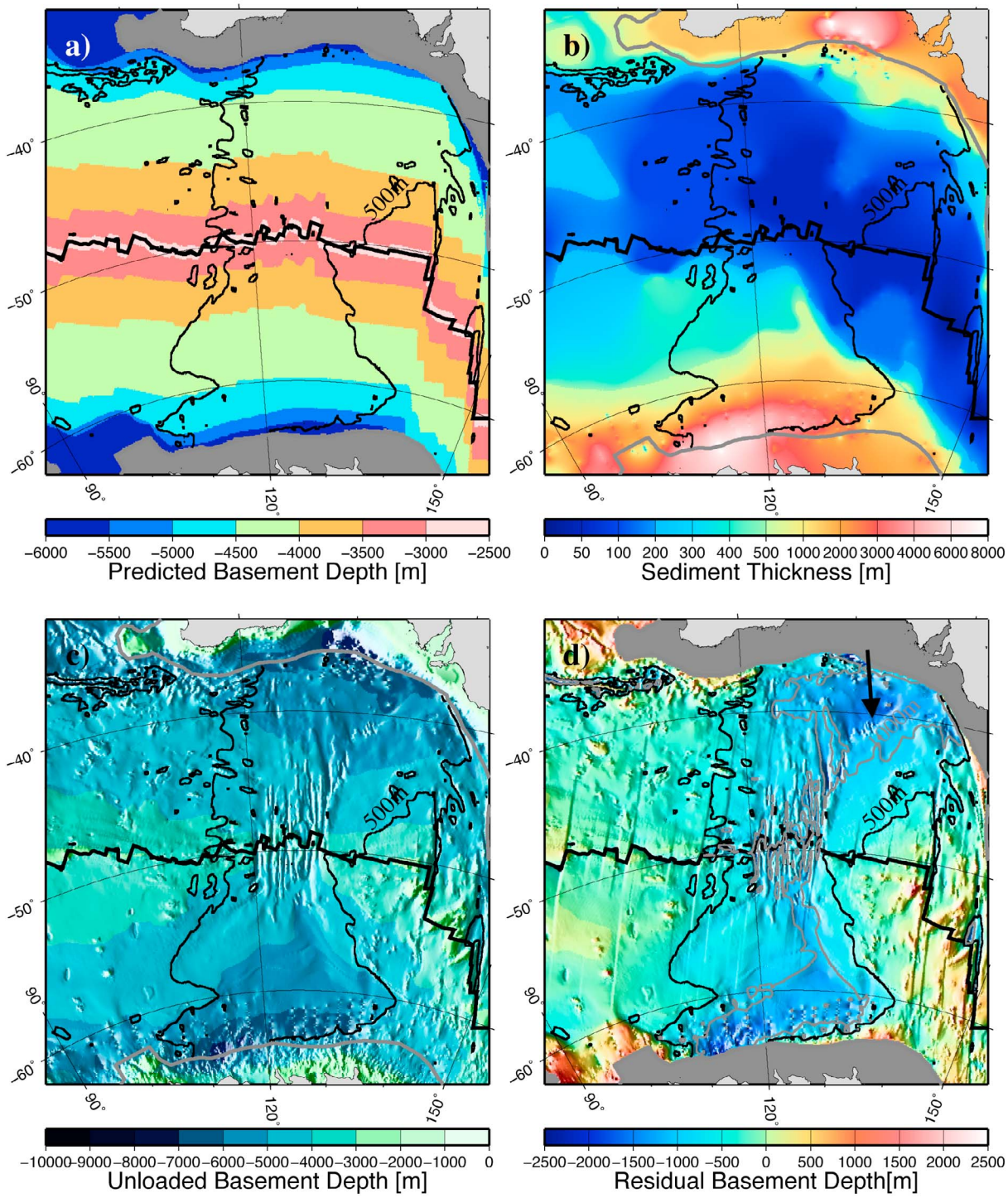

Figure 4. Regional maps showing (a) a predicted basement depth grid based on the thermal boundary layer depth-age relationship from *Pribac* [1991] (2600 + 315Age$^{1/2}$); (b) sediment thickness from *Géli et al.* [2007] combined with gridded sediment thickness interpreted from the seismic profiles in the Great Australian Bight and off Wilkes land shown in Figure 1 and the NGDC sediment thickness grid [*Divins*, 2004]; (c) unloaded basement depth from combining etopo2 bathymetry [*National Geophysical Data Center*, 2006] with sediment thickness from Figure 4b, using an isostatic correction after *Sykes* [1996]; and (d) residual depth anomaly between Australia and Antarctica, based on our unloaded basement depth grid (Figure 4c) and a predicted depth grid based on the thermal boundary layer depth-age relationship (Figure 4a). Residual depth anomaly contours at 500 m (black) and 1000 m (gray). Black arrow shows location of sharp gradient in the residual depth anomaly grid.

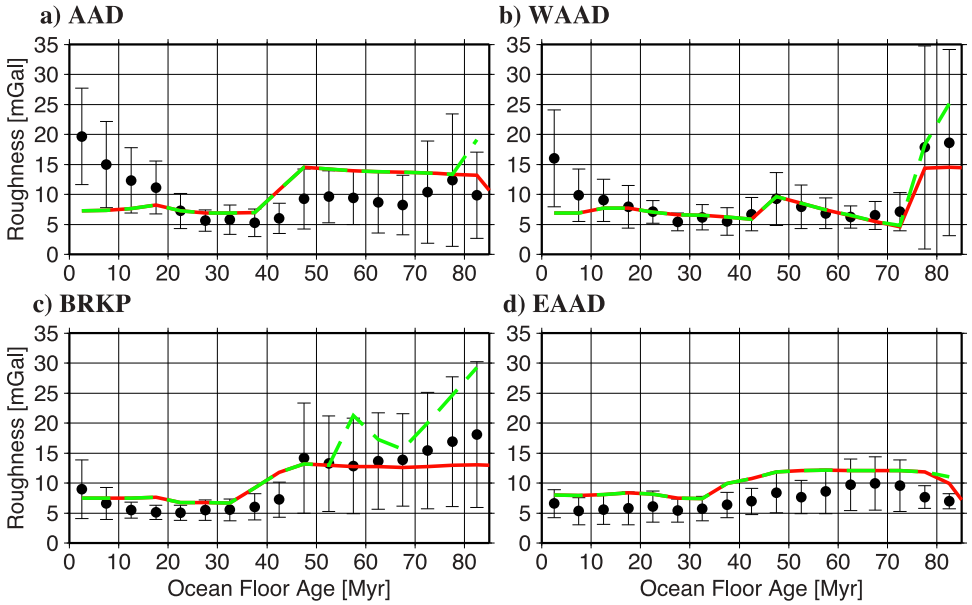

Figure 5. Gravity roughness as a function of seafloor age for four regions: (a) AAD, (b) WAAD, (c) BRKP, and (d) EAAD. Black dots and error bars show observed median roughness and its median absolute deviation in 5 Ma bins. The red line shows the roughness for each bin predicted based on the relationship between half-spreading rate and roughness and sediment thickness and roughness from *Whittaker et al.* [2008], and green lines shows roughness predicted based on sediment thickness, spreading rate, and spreading obliquity. Note the misfit between observed and predicted roughness for ocean crust formed <20 Ma in the AAD and WAAD.

Indian Ridge to approximately chron 6o (20.1 Ma) [*Müller et al.*, 2008]. Basement morphologies in adjacent, older crust are less rough and have more typical "abyssal plain" morphologies, similar to the majority of basement in the BRKP and EAAD regions. Oceanic crust proximal to the Australian southern margin is also rougher than adjacent younger basement (Figure 2). The purpose of our analysis is to remove roughness attributable to variations in spreading rate, sediment cover, and spreading obliquity in order to reveal oceanic basement that is anomalously rough. The presence of anomalously rough basement indicates the influence of anomalous mantle temperature and/or mantle fertility [*Whittaker et al.*, 2008].

[22] Estimates of oceanic basement roughness, based on spreading rate and sediment thickness, closely match predicted basement roughness for the regions analyzed here (red lines, Figure 5). One surprising result is that crust aged 50–83 Myr, proximal to both the Australian and Antarctica margins, exhibits high roughness amplitudes (Figure 2), but is not anomalously rough (Figure 5). The high roughness values are accounted for by the slow and oblique spreading prior to ~43 Ma (<10 mm/yr half-spreading rate). Slow and ultraslow spreading rates are known to result in rough oceanic basement which has been attributed to decreasing melt availability at slower spreading rates [*Chen and Phipps-Morgan*, 1996] and enhancement of the episodic magmatism and tectonic processes at mid-ocean ridges [*Malinverno and Pockalny*, 1990].

[23] Basement older than 75 Ma in the BRKP and the WAAD is rougher than predicted based on spreading rates and sediment thicknesses (red lines in Figures 5b and 5c). However, the roughness of these regions is more than accounted for when spreading obliquity is included (green dashed lines, Figure 5). Spreading obliquities >45° are related to increased roughness of oceanic basement, most likely due to an increase in brittle fracturing [*Whittaker et al.*, 2008]. Early opening between Australia and Antarctica has been modeled as highly oblique [*Whittaker et al.*, 2007]. Moreover, spreading prior to ~50 Ma was more oblique in the west compared to the east. This phenomenon likely explains the presence of the extremely rough Diamantina Zone (see Figure 1 for location) offshore southwest Australia, and why the elevated roughness decreases to the east. Close examination of Antarctic basement profiles, interpreted from multichannel seismic profiles (Figures 6 and 7), reveals the change in basement character from west to east caused by the slower and more oblique

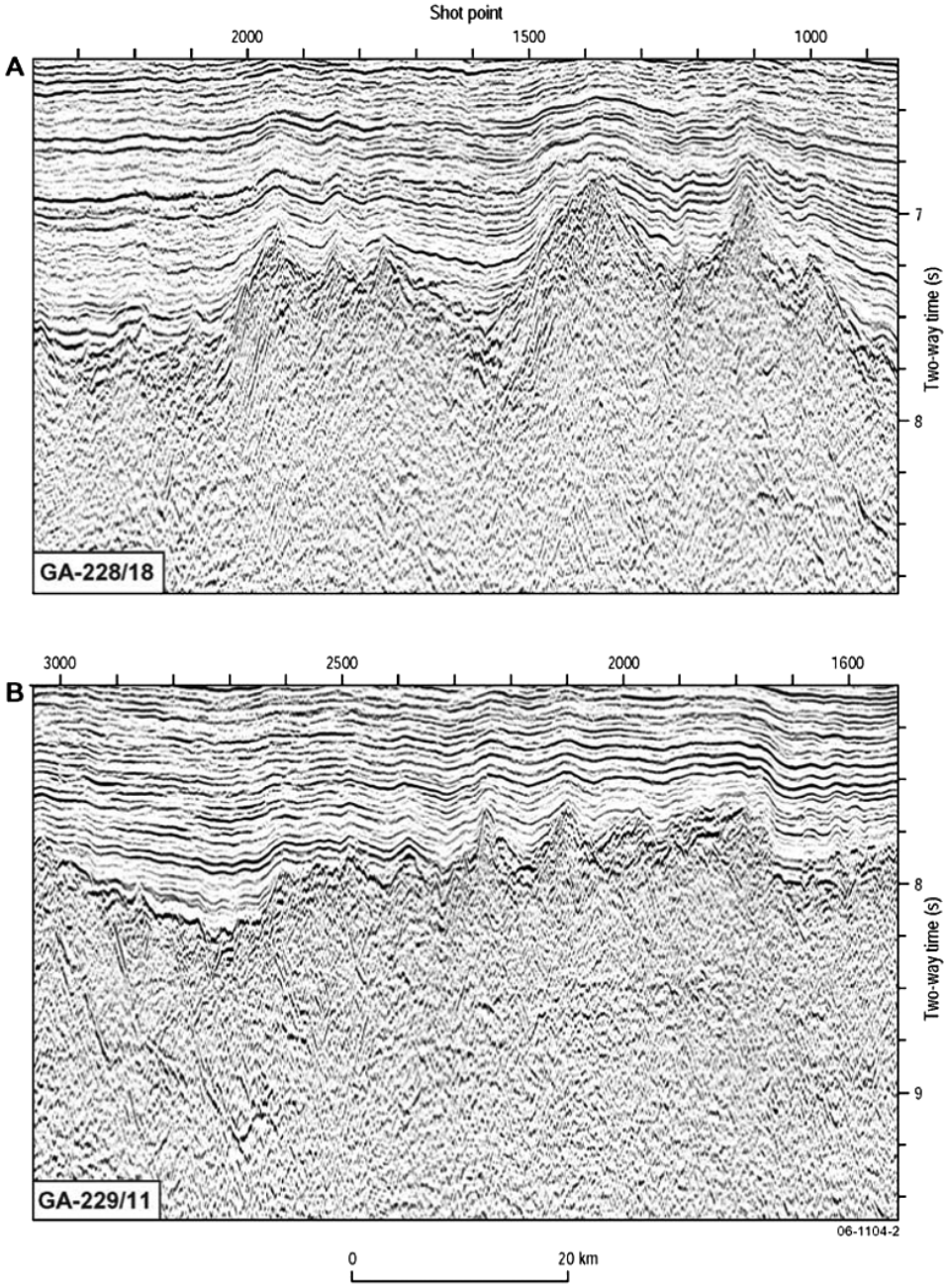

Figure 6. Selected seismic profiles illustrating characteristics of oceanic crust along strike of the Antarctic margin. (a) Line GA-228/18, west Wilkes Land (corresponds to central part of profile 5 in Figures 1 and 7). (b) Line GA-229/11, central Wilkes Land (corresponds to central part of profile 10 in Figures 1 and 7). (c) Line GA-228/23, central Wilkes Land (corresponds to central part of profile 14 in Figures 1 and 7). (d) Line GA-228/28, east Wilkes Land (corresponds to central part of profile 19 in Figures 1 and 7).

spreading. To the west, basement inboard of chron 20o shows higher-amplitude, longer-wavelength morphologies which decrease toward the east into lower-amplitude, shorter-wavelength basement morphologies.

[24] It is possible that the oceanic crust proximal to the margins appears less rough than it should due to attenuation of satellite-derived gravity roughness for areas of deep bathymetry. However, we have attempted to minimize this effect by downward

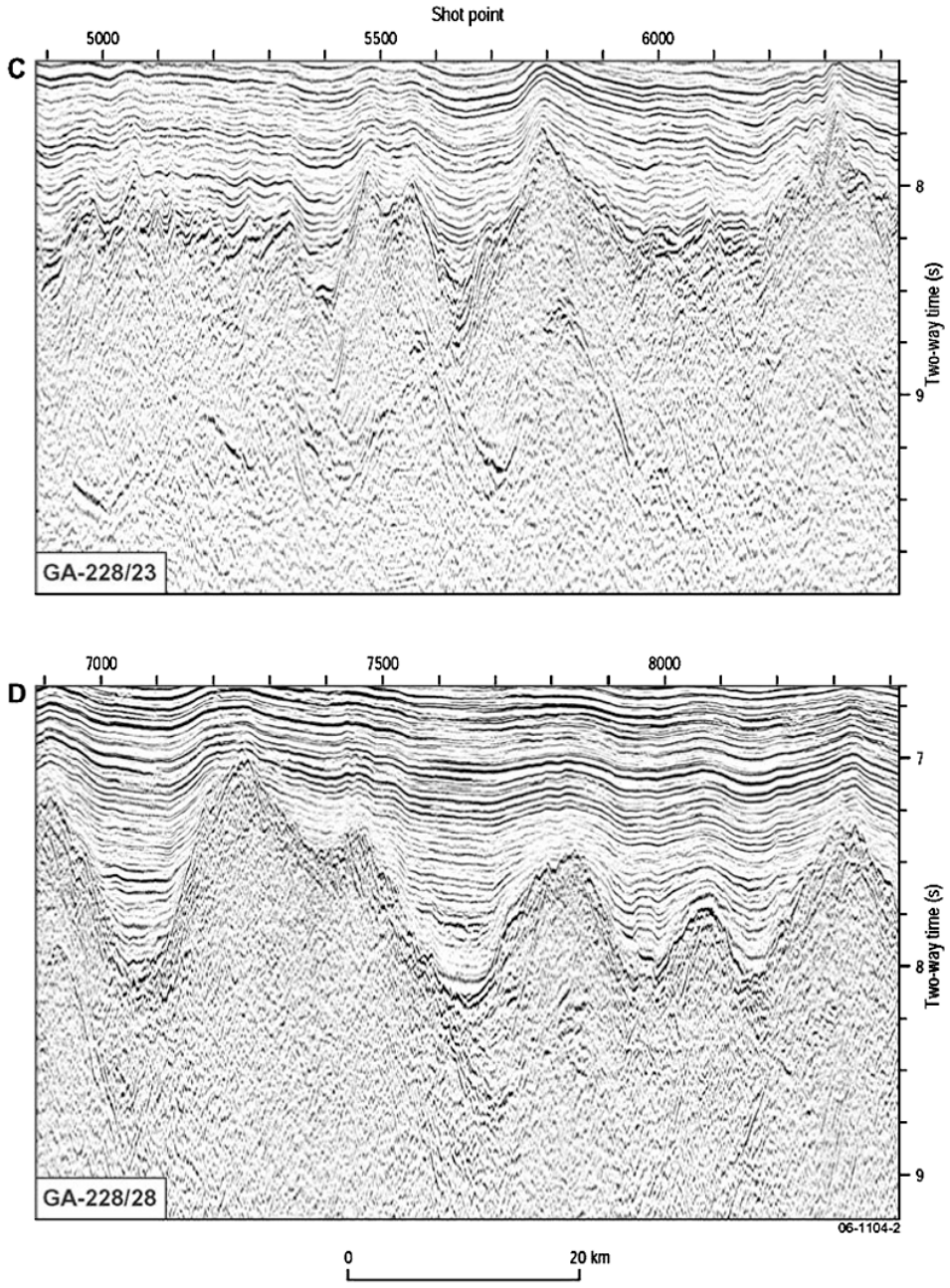

Figure 6. (continued)

continuing the satellite gravity to the seafloor. A global analysis of the relationship between RMS roughness and bathymetry (Figure S1 in the auxiliary material) indicates that there is only a very mild relationship between increasing depth and smoother basement, ~4 mGal of smoothing for an increase of ~3000 m of water depth.[1]

[25] Oceanic basement roughness values throughout the EAAD region are smoother than expected based on spreading rates and sediment thickness (Figure 5d). This result is consistent with results from the North and South Pacific which exhibit oceanic crust that is smoother than the global average [*Whittaker et al.*, 2008]. The EAAD portion of the Southeast Indian Ridge currently overlies Pacific-type mantle [*Christie et al.*, 2004; *Kempton*

[1]Auxiliary materials are available in the HTML. doi:10.1029/2010GC003276.

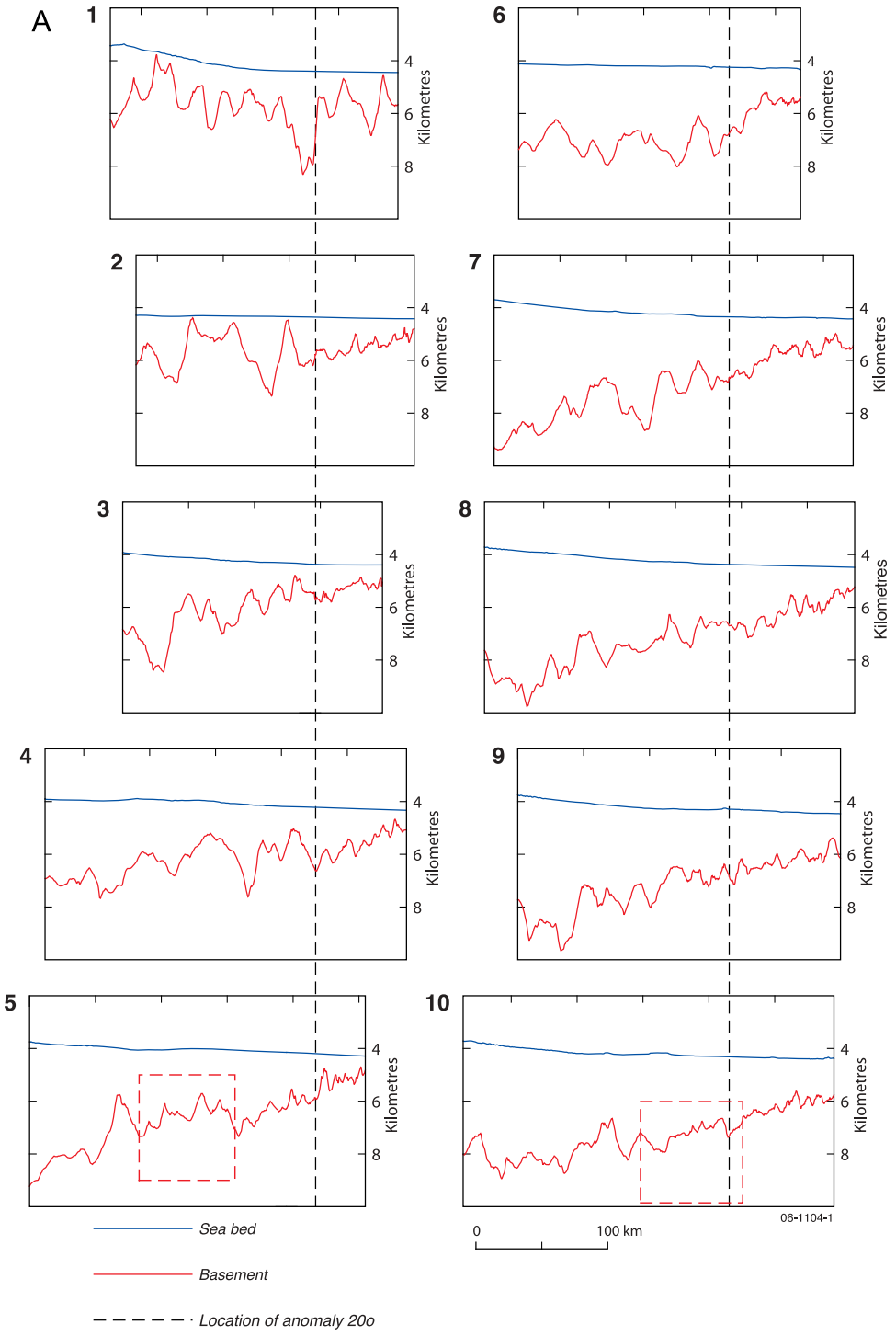

Figure 7. Profiles of water depth and depth to basement of the postrift section (i.e., depth to basement over oceanic crust) for the continental margin of (a) west and central Wilkes Land and (b) central Wilkes Land to Terre Adélie. Profile numbers correspond to numbered profiles on Figure 1. Depth conversion was carried out using smoothed stacking velocities and used the interpretation contained by *Stagg et al.* [2005]. Profiles are aligned on seafloor spreading magnetic anomaly 20o (43.8 Ma [*Cande and Kent*, 1995]). The magnetic anomaly 20o alignment is extrapolated for profiles 1–4 as they do not cross this anomaly.

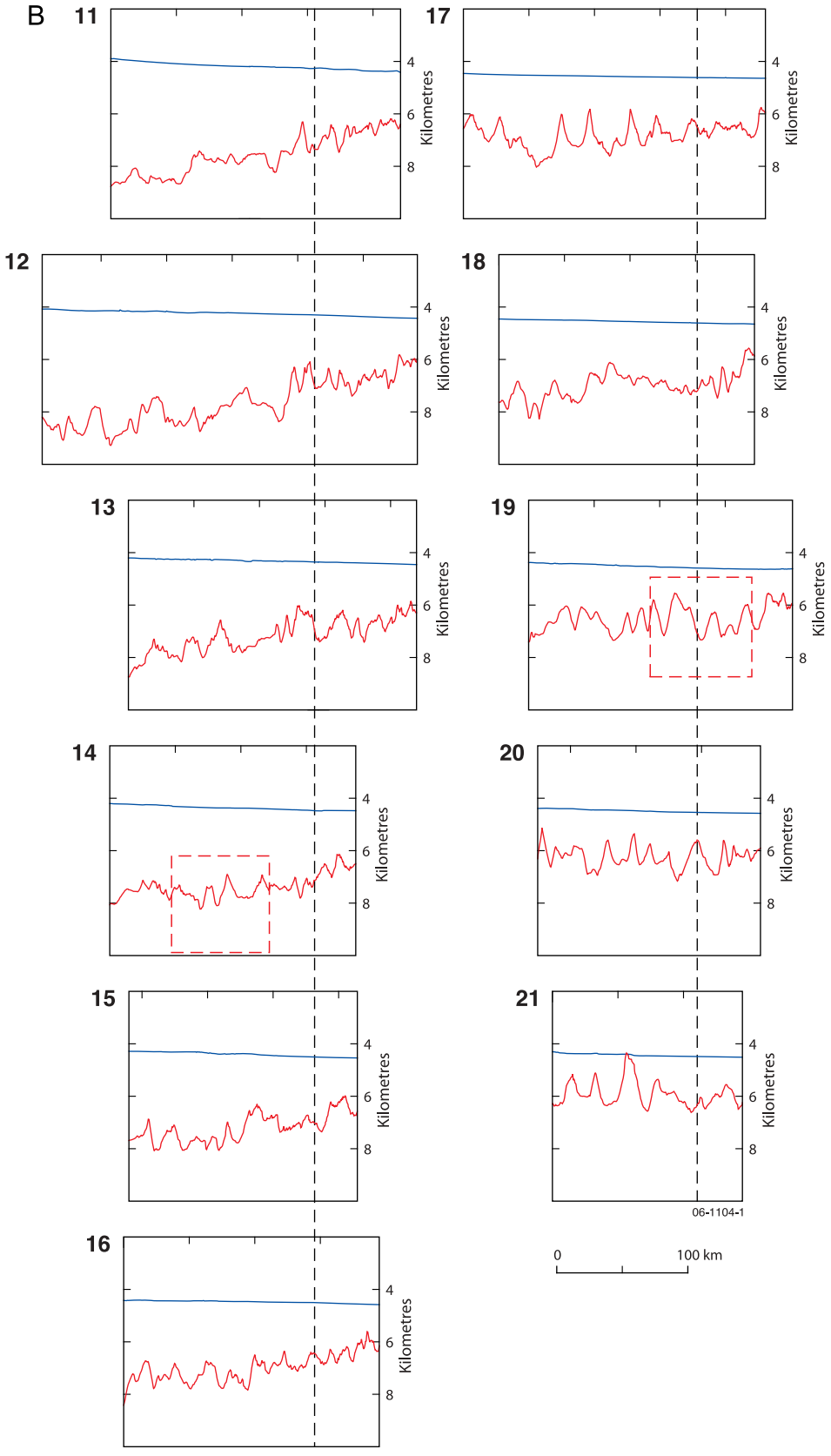

Figure 7. (continued)

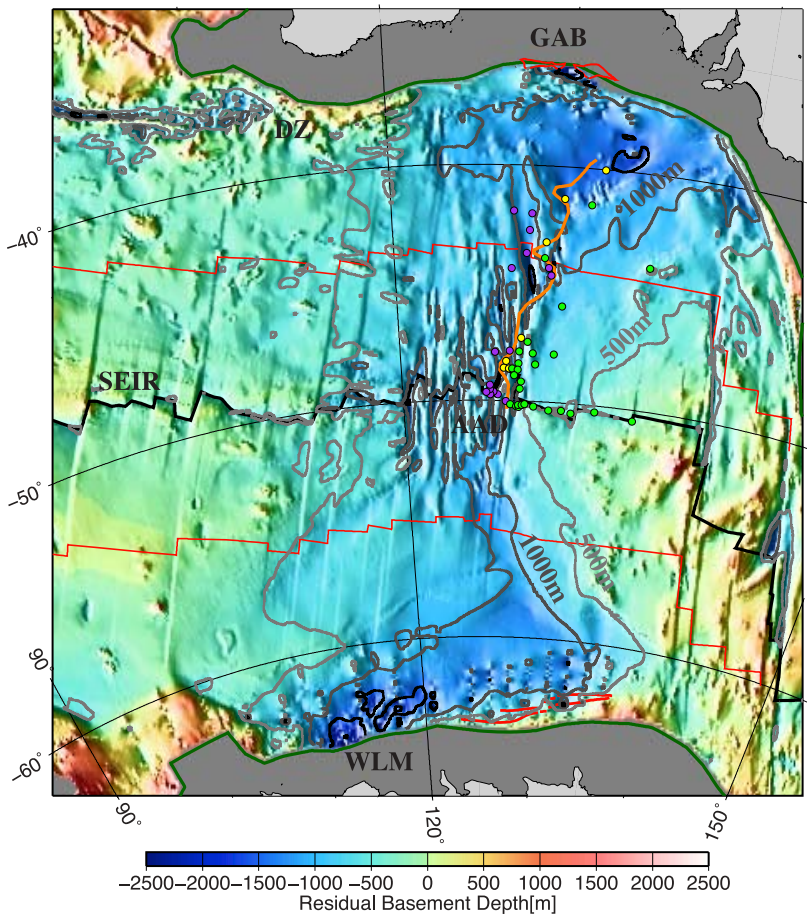

Figure 8. Residual depth anomaly (as in Figure 4d) between Australia and Antarctica based on unloaded basement depth (Figure 4c) and lithospheric cooling (Figure 4a). Residual depth anomaly contours are shown as 500 m (light gray), 1000 m (dark gray), and 1500 m (black). Basalt geochemistry data [*Christie et al.*, 2004; *Kempton et al.*, 2002] plotted as small circles for Pacific-type mantle source (green circles), mixed mantle source (yellow circles), and Indian mantle source (purple circles). Orange line shows boundary between Pacific- and Indian-type mantle [*Christie et al.*, 2004]. Continent-ocean boundaries are shown by green lines, peridotite ridges are shown by thick red lines, and 20 Ma isochron are shown by thin red lines.

et al., 2002]. The smooth oceanic basement throughout the EAAD suggests that this section of the Southeast Indian Ridge has sampled Pacific-type mantle since the onset of seafloor spreading between Australia and Antarctica at ~83 Ma.

[26] Anomalously rough oceanic basement, where the roughness is not explained by spreading rate, spreading obliquity and sediment thickness variations, occurs for oceanic crust younger than ~20 Ma in the AAD, and younger than ~15 Ma in the WAAD (Figures 5a and 5b). The unusual morphologies of the oceanic basement straddling the Southeast Indian Ridge in the AAD region have long been recognized, however, the onset of these morphologies has not been well defined. *Marks et al.* [1999] found that the crenulated bathymetry of the AAD started to develop at about 20 Ma while *Christie et al.* [1998] argued that "chaotic" basement fabrics extended to 30 Ma, based on analysis of swath bathymetry. Our results (Figures 5a and 5b) indicate that formation of rough oceanic basement began in the AAD at ~20 Ma and the WAAD from 15 Ma. Our analysis is regional in nature and while it does not support the formation of rough basement morphologies, it is possible that localized areas of "chaotic" basement may have formed prior to ~20 Ma, as described by *Christie et al.* [1998].

[27] A broad area of the Southern Ocean between Australia and Antarctica has a residual depth anomaly of at least 500 m (Figures 4d and 8), in contrast to the anomalous roughness, which is spatially restricted. The western extent of the 500 m depth anomaly roughly traces a prominent fracture zone

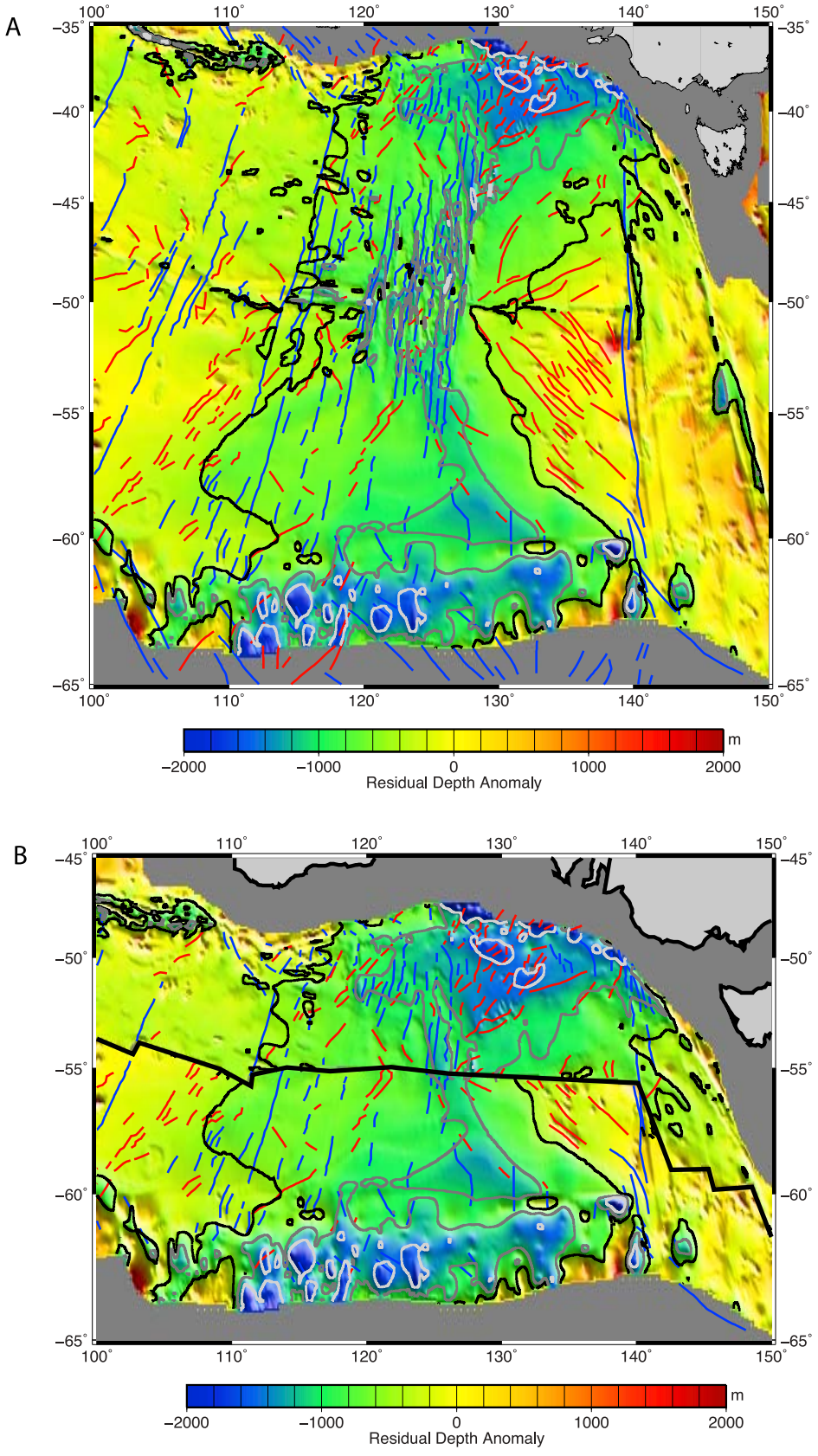
A
100°
110°
120°
130°
140°
150°
−35°
−40°
−45°
−50°
−55°
−60°
−65°
m
−2000
−1000
0
1000
2000
Residual Depth Anomaly
B
100°
110°
120°
130°
140°
150°
−45°
−50°
−55°
−60°
−65°
m
−2000
−1000
0
1000
2000
Residual Depth Anomaly

Figure 9

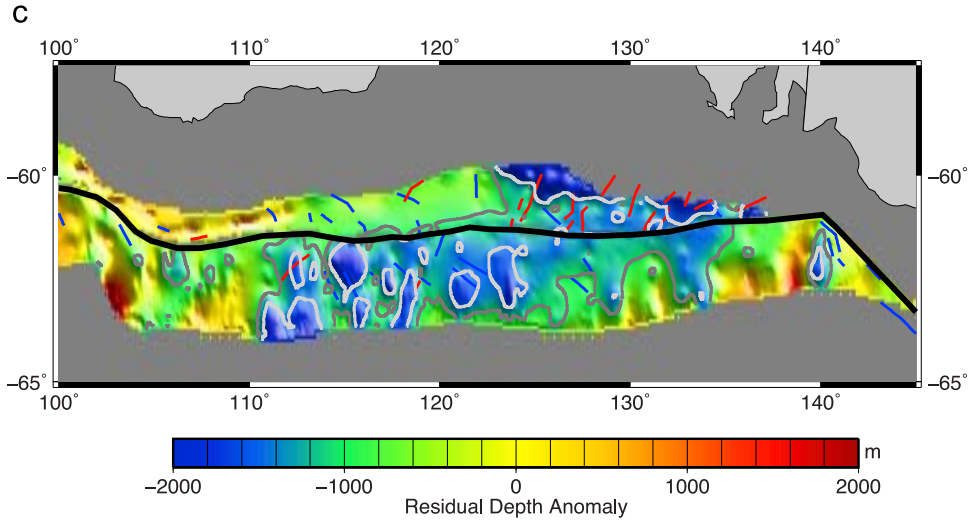

Figure 9. (continued)

that intersects the Southeast Indian Ridge at ~114° E. Previously, *Christie et al.* [1998], *Gurnis and Müller* [2003], *Marks et al.* [1990], and others have described the eastern boundary of the 500 m RDA as a symmetric, westward pointing V-shaped geometry, which is in agreement with our results. However, our 500 m contour is located ~70–400 km further east compared with the 600 m residual depth anomaly contour of *Marks et al.* [1990], which is more closely correlated with our 1000 m contour (Figure 8). The difference is due to a number of factors. *Marks et al.* [1990] used the *Turcotte and Oxburgh* [1967] thermal boundary layer model of depth-age relation, while we used the *Pribac* [1991] model that was developed specifically for the oceanic basement of the Australian Southern Ocean. *Marks et al.* [1990] used nearly 60,000 km of ship track bathymetric data while we utilize modern 1m bathymetric data inferred from satellite gravity. *Marks et al.* [1990] estimated sediment thicknesses from available seismic data and removed the sediment cover using a uniform sediment density of 1900 kg m^{-3}. The available coverage of sediment thickness data has improved markedly since *Marks et al.* [1990] and we also unloaded the improved sediment thickness data taking into account density changes related to total sediment thickness [*Sykes*, 1996], as opposed to using an assumed average density for the entire sedimentary succession independent of its thickness.

[28] *Gurnis and Müller* [2003] noted the highly symmetric nature of the 500 m RDA and described the spatial extent as "hourglass" in shape. Our results also show the symmetric nature of the 500 m RDA, but we find the anomaly to be V shaped only on the eastern boundary. The western boundary, by contrast, is more linear and roughly follows the fracture zone trend. Indeed, the 500 m RDA is more "K shaped," than "V" or "hourglass" shaped. The 500 m RDA contour is roughly symmetric in Figures 8 and 9a, however when reconstructed to 20 Ma the 500 m contour shows a striking asymmetry on the eastern boundary of the AAD. By comparison, the 1000 m RDA is broadly symmetric when reconstructed at 20 Ma.

[29] Within the 500 m RDA there are three areas of particularly deep oceanic basement. These are the 0–20 Ma crust formed within the AAD, which has residual depth anomalies of >1000 m, and the <~40 Ma crust proximal to the Australian and Antarctic continental margins with residual depth anomalies >1500 m.

[30] The residual depth anomaly deepens and widens toward the continental margins (Figure 8), in agreement with previous results [e.g., *Cochran and Talwani*, 1977; *Gurnis and Müller*, 2003; *Marks et al.*, 1999; *Veevers*, 1982]. Proximal to both the Antarctic and Australian margins, residual

Figure 9. Residual depth anomaly between Australia and Antarctica at (a) 0Ma, (b) 20.1 Ma, and (c) 47.9 Ma. Thick black line shows the location of the Southeast Indian Ridge. Residual depth anomaly contours are shown as 500 m (black), 1000 m (gray), and 1500 m (light gray). Fracture zones (blue) and other tectonic lineaments (red) interpreted from satellite free-air gravity are also shown.

depth anomalies of >1000 m extend 1600–1900 km across both margins, and contain pockets of residual depth anomalies of >1500 m. The residual depth anomalies >1000 m are predominantly found in oceanic crust formed between 40 and 83 Ma, although the Australian anomaly extends further offshore affecting crust with ages up to 30 Ma (Figure 8). Proximal to the Australian margin the 1000 m and 1500 m depth anomalies occur adjacent to the Great Australian Bight, extending over ~1300 km and ~650 km, respectively. Adjacent to the Wilkes Land margin the 1000 m and 1500 m depth anomalies extend over ~1300 km and ~515 km, respectively.

[31] One important observation is that the transition to the 1000 m depth anomaly is steeper on the eastern side compared to the western. This can be observed in Figure 4d and is particularly apparent on the Australian margin, at approximately 40°S, 135°E.

4. Discussion

4.1. AAD Oceanic Basement Younger Than 20 Ma

[32] Young (<20 Ma) oceanic crust in the AAD and WAAD is anomalously rough and deep (500 m to >1000 m) but is surrounded by crust that is only anomalously deep (~500 m). *Montési and Behn* [2007] argue that reduced melt volumes cause episodic volcanism and alternating periods of crustal extension and accretion, leading to the formation of rough and deep oceanic basement. During amagmatic periods the newly formed ocean crust proximal to the ridge undergoes extension leading to rougher basement morphologies and thinner, and hence deeper, oceanic basement.

[33] Two mechanisms are known to reduce magma supply beneath a mid-ocean ridge, resulting in changes in mid-ocean ridge morphologies and roughness: (1) slow (<20 mm/yr) half-spreading rates [*Malinverno*, 1991; *Small and Sandwell*, 1989; *Smith*, 1998; *Whittaker et al.*, 2008] and (2) cool and/or depleted upper mantle [*Klein and Langmuir*, 1987; *Meyzen et al.*, 2003].

[34] The Southeast Indian Ridge has experienced moderate spreading rates (37 mm/yr) since ~43 Ma, so it is clear that slow <20 mm/yr spreading rates are not the primary cause of the young, deep oceanic basement observed in the AAD and WAAD. The only viable alternative is that cool and/or depleted upper mantle material has been sampled by the Southeast Indian Ridge since ~20 Ma.

[35] There is substantial support for the presence of cool upper mantle beneath the AAD. Regional analysis of surface waves [*Forsyth et al.*, 1987; *Kuo et al.*, 1996, 1984] and global inversions [*Masters et al.*, 2000; *Mégnin and Romanowicz*, 2000; *Ritsema and Van Heijst*, 2000; *Ritzwoller et al.*, 2003; *Zhang and Tanimoto*, 1993] reveal larger than normal seismic velocities in the AAD upper mantle. Basalt petrology results are also consistent with the presence of cool upper mantle material [*Bown and White*, 1995a, 1995b; *Klein and Langmuir*, 1987].

[36] *Ritzwoller et al.* [2003] imaged a NW–SE trending anomaly beneath the AAD in the upper 120 km of mantle and proposed that the restricted extent of this anomalous body meant that northward absolute motion of the Southeast Indian Ridge over this feature could account for the onset of AAD basement morphologies at ~20 Ma [*Ritzwoller et al.*, 2003]. However, this interpretation implies that the anomalous upper mantle body has remained in the upper mantle since the extinction of the westward dipping Mesozoic subduction zone, an unlikely scenario given the time scales involved. An alternative hypothesis [*Gurnis et al.*, 1998] is that this body has been progressively drawn up beneath the Southeast Indian Ridge, and has been sampled by the northward migrating Southeast Indian Ridge since ~20 Ma.

[37] Sampling of cool and/or depleted upper mantle is consistent with the thin oceanic crust observed within the AAD. Based on ridge proximal data, thickness of AAD oceanic crust gradually decreases from west to east at a rate of 0.1km/100 km [*Holmes et al.*, 2008] and then rapidly increases across the eastern AAD boundary from ~4.8 km to 7.3 km over a distance of ~50 km [*Holmes et al.*, 2010]. *Holmes et al.* [2010] proposed that that the AAD is the surface expression of a terminal end to a long-wavelength reduction in melt supply, and that the rapid increase in crustal thickness at the eastern boundary of the AAD is related to the boundary between Indian- and Pacific-type mantle.

[38] There is some dispute as to whether the upper mantle anomaly can entirely explain the residual depth anomalies observed in the <20 Ma AAD. *Ritzwoller et al.* [2003] proposed that depressed mantle temperatures of ~100°C (and up to 200°C) [*Ritzwoller et al.*, 2003] are qualitatively sufficient to result in the observed depth anomaly variations and oceanic crust that is 2–4 km thinner than normal

[*Tolstoy et al.*, 1995]. In comparison, *Gurnis et al.* [1998] computed that anomalously thin 3.6–4.2 km oceanic crust proximal to the Southeast Indian Ridge [*Tolstoy et al.*, 1995] accounts for only ~50% of a ~800 m depth anomaly in oceanic crust younger than ~20 Ma. Our analysis finds that AAD basement younger than 20 Ma exhibits residual depth anomalies >1000 m, at least 200 m more than the analysis of *Gurnis et al.* [1998], due to differences in the quality of available bathymetric and sediment data and sediment unloading calculations (see section 3 for a more detailed discussion). This implies that anomalously thin crust accounts for less than 50% of the depth anomaly. *Gurnis et al.* [1998] proposed that negative dynamic topography, due to the sinking ancient slab at depth, is responsible for the remaining depth anomaly.

[39] Proximal to the Southeast Indian Ridge, roughly N–S linear 1000 m RDA contours, that are coincident with fracture zones, are observed (Figure 8). This observation is related to the presence of thinner crust proximal to the fracture zones. Melt migrating laterally along the fracture zone, rather than building up the lower crust, is thought to result in anomalously thin crust proximal to fracture zones, commonly half as thick as adjacent crust [*White et al.*, 1992]. Such a phenomenon has been imaged at the slow spreading Mid-Atlantic Ridge where a 3D flow pattern has resulted in thinner crust at fracture zones and centralized upwelling near segment centers [*Barth and Mutter*, 1996].

[40] Geochemical data obtained from dredges and Leg 187 of the Ocean Drilling Program [*Christie et al.*, 2004; *Kempton et al.*, 2002] have enabled the boundary between Indian-type and Pacific-type mantle to be clearly delineated beneath oceanic crust younger than ~28 Ma in the Australian Southern Ocean (see Figure 8). The implication is that Indian-type mantle underlies the AAD to the west of this boundary and Pacific-type mantle occurs to the east of this boundary. For basement younger than ~20–30 Ma, this clearly defined geochemical boundary corresponds with the sharp eastern boundary of our 1000 m RDA contour. The arcuate shape of both these features is most likely linked to the encroachment of Pacific-type mantle at a rate of ~1.5 mm/yr since ~28 Ma [*Christie et al.*, 2004; *Kempton et al.*, 2002]. The very rapid gradient of the RDA on the eastern boundary of the AAD, and the corresponding rapid change in crustal thickness from ~4.8 km (west) to 7.3 km (east) over a distance of ~50 km is almost certainly caused by the underlying transition from cool/depleted Indian-type mantle with subducted slab affinities beneath the AAD to more typical Pacific-type mantle to the east.

[41] The eastern boundary of the 500 m RDA contour is V shaped and is located wholly above Pacific-type mantle some ~70–400 km east of the Indian-Pacific mantle boundary, where crustal thickness are observed to be ~7.3 km [*Holmes et al.*, 2010]. It is therefore highly unlikely that the distinctive V-shaped 500 m RDA is a result of geochemical differences in the mantle. However, the 500 m RDA contour does show a clear relationship with the trace of westward propagating ridges (see Figures 8 and 9). Particularly on the Antarctic flank, the 500 m RDA contour marks the boundary between oceanic crust exhibiting typical abyssal hill fabrics (west) and propagating ridge traces (east). Propagating ridges are usually associated with relatively high magma supply however, the propagating ridges of this section of the Southeast Indian Ridge are unusual, with crustal thickness variations and westward subaxial asthenospheric flow proposed as the main driving mechanisms [*West et al.*, 1999]. When reconstructed to 20 Ma, a considerable offset is apparent in eastern boundary of the 500 m RDA between the northern and southern flanks of the Southeast Indian Ridge (Figure 9b). This distinctive asymmetry indicates that mid-ocean ridge processes alone are unlikely to be responsible for forming the V-shaped residual depth anomaly, and that more recent asthenospheric flows beneath this portion of the Southeast Indian Ridge, to the east of the AAD, are resulting in a positive residual depth anomaly effect. Some of the asymmetry observed both at the present day and at 20 Ma is likely a result of the westward propagating ridges leading to the accretion of more oceanic lithosphere on the northern flank of the Southeast Indian Ridge (Figure 8). Therefore, we propose that the distinctive V shape of the 500 m RDA is related to westward mantle flow, within the Pacific-type mantle domain.

[42] In contrast to the eastern boundary of the 500 m RDA, the western boundary is roughly linear and follows the NNE strike of the fracture zones at ~114°E. *Holmes et al.* [2008] found no dramatic change in crustal thicknesses across this western boundary, instead reporting a gradual decrease in thickness from ~6 km at 100°E to ~5 km at 115°E, a trend which appears to continue eastward across the AAD [*Holmes et al.*, 2010]. On the basis of this data *Holmes et al.* [2010] propose that mantle beneath the AAD becomes increasingly depleted toward the east and that the rapid changes in AAD basement morphology are the result of crossing a

mantle depletion threshold. We agree that it is most likely that the transition to rough AAD basement morphologies is related to the crossing of a mantle threshold that controls crust accumulation processes at intermediate rate spreading ridges. However, seismic tomography results [e.g., *Ritzwoller et al.*, 2003] reveal the presence of a cool mantle body beneath the AAD portion of the Southeast Indian Ridge, the formation of which is not explained by the inhibited mantle replenishment hypothesis [*Buck et al.*, 2009; *Holmes et al.*, 2010]. We propose that the mantle variations are more likely related to the upwelling and mixing of slab related mantle with Indian-type mantle.

[43] We also propose that the western boundary of the 500 m RDA contour is related to the long-wavelength negative dynamic topography signal caused by the ancient subducted slab at depth. A negative dynamic topography component is required to explain the large (>1000 m) residual depth anomalies observed within the AAD [*Gurnis et al.*, 1998]. There is substantial evidence for the presence of such a cold body. Seismic shear velocity anomalies from different global seismic inversion models, SB4L18 [*Masters et al.*, 2000], SAW24B16 [*Mégnin and Romanowicz*, 2000], and S20RTS [*Ritsema and Van Heijst*, 2000] all support the presence of a N–S to NW–SE oriented seismically fast (cold) zone at depth. Negative dynamic topography is also apparently the only way to explain why the 500 m RDA contour extends so far east, affecting crust with normal crustal thicknesses, ~7.3 km [*Holmes et al.*, 2010], overlying Pacific-type mantle. We suggest that the negative dynamic topography effect of the ancient subducted slab extends from ~114°E to ~140°E, the westernmost and easternmost extents of the 500 m RDA contour. In the east, we propose that westward propagating buoyant Pacific-type asthenospheric mantle flow, wholly within the Pacific mantle domain, is responsible for overprinting the negative dynamic topography signal, resulting in the propagating ridges of the EAAD and the V-shaped 500 m RDA.

4.2. AAD Oceanic Basement Older Than 20 Ma

[44] A key observation arising from our analysis is that regions of anomalous roughness are spatially limited to basement that is younger than 20 Ma, whereas anomalous residual depths affect a broad region of oceanic basement aged 0–83 Ma, and also potentially onshore. Further, the residual depth anomaly deepens and widens toward the continental margins (Figure 8), in agreement with previous results [e.g., *Cochran and Talwani*, 1977; *Gurnis and Müller*, 2003; *Marks et al.*, 1999; *Veevers*, 1982].

[45] The different spatial extents of the residual depth anomaly and rough basement morphologies have been noted previously [*Christie et al.*, 2004; *Gurnis and Müller*, 2003; *Marks et al.*, 1999] based on residual depth anomalies, geochemistry and basement morphology. Any model attempting to explain the formation of oceanic basement in the Australian Southern Ocean must address the different spatial distributions of these phenomena. We propose that three mechanisms, negative dynamic topography, sampling of anomalous mantle, and ultralow spreading rates, have all influenced the AAD, resulting the complex geological and geophysical patterns.

[46] Following the same arguments outlined in section 4.1, we propose that the subducted Mesozoic slab at depth results in negative dynamic topography that extends across the Southern Ocean (and possibly onshore) from the linear western boundary of the 500 RDA to approximately ~140°E. Figure 8 shows that the 500 m RDA extends east past the Indian-Pacific geochemical boundary, affecting normal thickness oceanic basement overlying unaltered Pacific-type mantle. This indicates the influence of a dynamic topography mechanism rather than a crustal thickness mechanism for the residual depth anomalies in this region.

[47] Another mechanism that likely played a role in forming the broad, >1500 m RDAs proximal to the Australian and Antarctic margins are ultraslow spreading rates. At half-spreading rates >~10 mm/yr crustal thicknesses are relatively constant at 7.1 ± 0.9 km [*Bown and White*, 1994; *White et al.*, 1992]. In contrast, oceanic crust formed at very slow spreading rates (<10 mm/yr) is anomalously thin and exhibits unusually small amounts of melt generation [*White et al.*, 1992]. The major difference is in Layer 3, which is much thinner than normal under very slow spreading conditions [*Muller et al.*, 1999]. The spreading rates as Australia and Antarctica separated from ~83 Ma to ~43 Ma were extremely slow (<10 mm/yr) and highly oblique [*Whittaker et al.*, 2007]. As a result, oceanic crust older than ~43 Ma can be expected to be thinner, and thus deeper, than younger crust in the AAD. However, the residual basement depths are not consistently deep along the Australian or Antarctic margin.

[48] In fact, the deepest residual basement depths occur in relatively narrow pockets on both margins.

On the Australian margin the deepest residual depth anomalies occur immediately west of the Indian-Pacific geochemical boundary and are bounded on the eastern side by particularly sharp gradients (Figures 4 and 8, black arrow) that are proximal to the Indian-Pacific geochemical boundary (Figure 8) across which rapid crustal thickness variations occur [*Holmes et al.*, 2010]. These observations cannot be explained by the combination of negative dynamic topography and ultraslow spreading rates. Negative dynamic topography does not affect crustal thickness and is highly unlikely to result in sharp topographic gradients. Ultraslow spreading rates affected the entire length of the conjugate Australian-Antarctic margins so are also highly unlikely to have resulted in a rapid change in crustal thickness. We propose that a subsection of the early, ultraslow spreading Southeast Indian Ridge, immediately to the west of the Indian-Pacific mantle boundary, sampled subduction wedge contaminated mantle resulting in the deepest margin proximal residual depth anomalies.

[49] Sampling of anomalous upper mantle has previously been proposed to explain the formation of the particularly deep oceanic crust proximal to both continental margins. *Gurnis and Müller* [2003] proposed that ancient mantle wedge material originating from a Mesozoic subduction zone remained in the upper mantle and was sampled by the Southeast Indian Ridge immediately following Australia-Antarctic breakup, leading to the formation of the large depth anomalies observed close to both margins through the formation of thin oceanic crust. This hypothesis, that mantle with a depleted mantle wedge component was sampled ahead of the upwelling cool mantle at ~20 Ma, is supported by interpretation of Nd-Hf isotope systematics from OPD Leg 187 recovered basalts [*Kempton et al.*, 2002]. They suggest that basalts within the AAD sampled a mantle source that originated as subduction-modified mantle wedge that was mixed back into the upper mantle beneath the Australian and Antarctic margin before the onset of rifting. Unfortunately, the samples used in this geochemical study did not extend into the most anomalous regions adjacent to the Australian margin.

[50] The presence of exhumed continental mantle on both the Australian [*Sayers et al.*, 2001] and Antarctic margins [*O'Brien and Stagg*, 2007] suggests that the combined influence of ultraslow spreading and anomalous upper mantle resulted in oceanic crustal accretion decreasing to zero during some periods of the early spreading history. However, an absence of oceanic crust cannot alone explain residual depth anomalies >1500 m. Computation of the crustal thickness from residual depth anomalies results in negative crustal thicknesses across the AAD, but particularly proximal to the margins (Figure 10). This result reveals that, alone, variations in crustal thickness are insufficient to account for the observed residual depth anomalies. It follows that negative dynamic topography, due to the presence of the ancient slab at depth, is also required to explain the >1500 m residual depth anomalies proximal to the margins.

[51] A problem with the involvement of depleted wedge contaminated mantle is that sampling of depleted mantle is observed to form oceanic basement that is anomalously rough as well as anomalously deep due to decreased crustal thicknesses [*Meyzen et al.*, 2003, 2005]. However, our results (Figures 5 and 8) show that while oceanic crust proximal to both the Australian and Antarctic margins is anomalously deep (>1500 m), it is not anomalously rough. The reason that there is no observed increase in basement roughness for these particularly deep regions could be because they have reached the upper limit of basement roughness caused by decreasing melt volumes and episodic magmatism induced by spreading rates and/or mantle temperatures. Below a threshold half-spreading rate value of ~15 mm/yr there was no increase in oceanic basement roughness [*Whittaker et al.*, 2007]. The implication is that the subduction wedge contaminated mantle resulted in an additional thinning of the oceanic crust without any increase in the roughness of the basement morphologies. Indeed, prominent basement ridges (Figures 1 and 8) of exhumed, serpentinized continental mantle [*O'Brien and Stagg*, 2007; *Sayers et al.*, 2001], indicative of the absence of oceanic basement and zero melt, are located within the deepest areas of residual bathymetry.

[52] The broadest and deepest, margin proximal residual depth anomalies (>1000 m) are predominantly found in oceanic crust formed between 40 and 83 Ma. In comparison, oceanic crust formed between ~40–20 Ma exhibits only a narrow, roughly N–S trending, band of residual depth anomaly greater than 1000 m (Figure 8). Elsewhere, oceanic basement formed between ~40–20 Ma is contained within the 500 m residual depth anomaly contour, which we propose is due to negative dynamic topography due to the Mesozoic slab material sinking in the mantle. The explanation for the presence of the deeper band of oceanic basement in the eastern portion of the 40–20 Ma AAD is likely due to either the presence of remnants of the

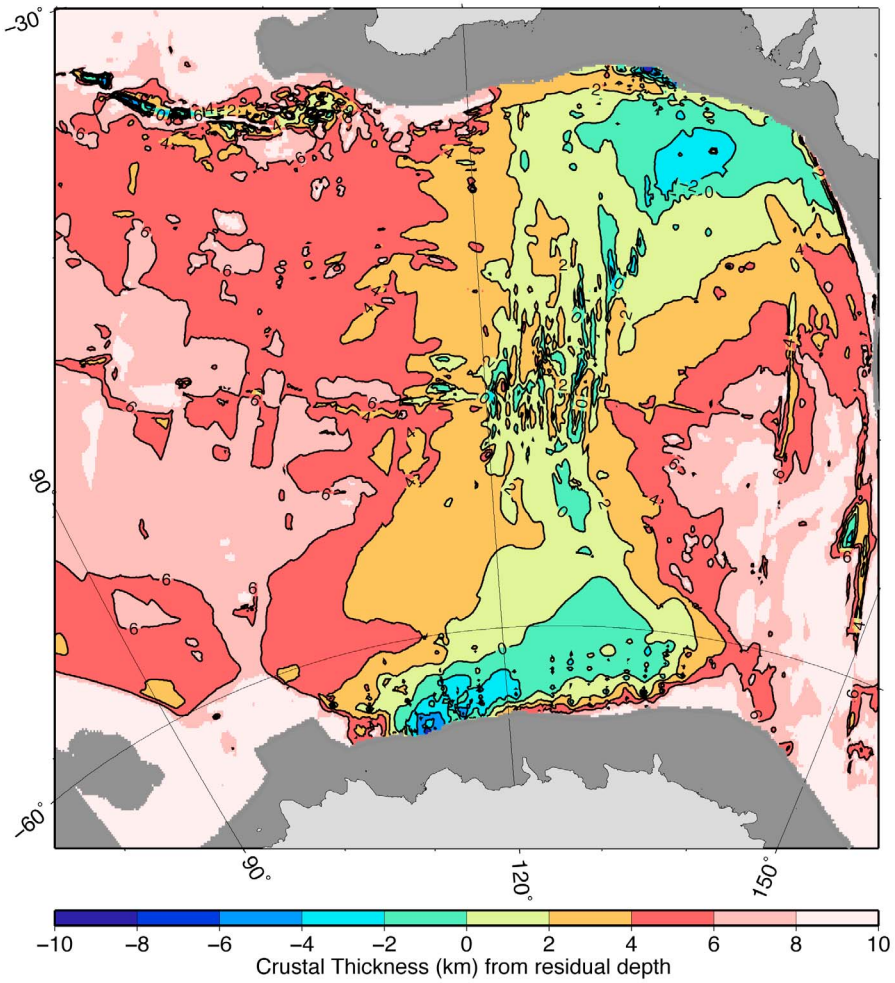

Figure 10. Computed crustal thickness based on the residual depth anomalies following the method of *Louden et al.* [2004]. This approach assumes that crustal thickness variations account for all residual depth anomaly variations. However, note the negative crustal thickness estimates proximal to the margins that indicate an additional mechanism is required.

mantle-wedge contaminated mantle responsible for the broad, margin proximal depth anomaly, or precursors of the upwelling mantle responsible for the young (<20 Ma) anomalous crust. The narrow eastern band of deeper oceanic basement also possibly exhibits rougher basement morphologies. Figure 1 shows two fracture zones extending into oceanic crust older than ~20 Ma and *Christie et al.* [1998] observed "chaotic" basement morphologies extending to crust aged ~30 Ma in the same area based on sparse multibeam data.

Acknowledgments

[53] Figures 1–5 and 8–10 were created using GMT [*Wessel and Smith*, 1991], and Figures 6 and 7 were provided by Geoscience Australia from material provided by H. Stagg. M.G. was partially supported by NSF grant EAR-0810303. We thank two anonymous reviewers for their helpful comments that greatly improved this paper, as well as the numerous people with whom we had helpful discussions, in particular H. Stagg (Geoscience Australia) and Simon Williams (University of Sydney).

References

Barth, G. A., and J. C. Mutter (1996), Variability in oceanic crustal thickness and structure: Multichannel seismic reflection results from the northern East Pacific Rise, *J. Geophys. Res.*, *101*, 17,951–17,975, doi:10.1029/96JB00814.

Bown, J. W., and R. S. White (1994), Variation with spreading rate of oceanic crustal thickness and geochemistry, *Earth Planet. Sci. Lett.*, *121*, 435–449, doi:10.1016/0012-821X(94)90082-5.

Bown, J. W., and R. S. White (1995a), Effect of finite extension rate on melt generation at rifted continental margins, *J. Geophys. Res.*, *100*, 18,011–18,029, doi:10.1029/94JB01478.

Bown, J. W., and R. S. White (1995b), Finite duration rifting, melting and subsidence at continental margins, in *Rifted Ocean-Continent Boundaries*, edited by E. Banda, pp. 31–54, Kluwer Acad., Dordrecht, Netherlands.

Buck, W., C. Small, and W. Ryan (2009), Constraints on asthenospheric flow from the depths of oceanic spreading centers: The East Pacific Rise and the Australian-Antarctic Discordance, *Geochem. Geophys. Geosyst.*, *10*, Q09007, doi:10.1029/2009GC002373.

Cande, S. C., and D. V. Kent (1995), Revised calibration of the geomagnetic polarity timescale for the Late Cretaceous and Cenozoic, *J. Geophys. Res.*, *100*, 6093–6095, doi:10.1029/94JB03098.

Chen, Y. J., and J. Phipps-Morgan (1996), The effects of spreading rate, the magma budget, and the geometry of magma emplacement on the axial heat flux at mid-ocean ridges, *J. Geophys. Res.*, *101*, 11,475–11,482, doi:10.1029/96JB00330.

Christie, D. M., B. P. West, D. G. Pyle, and B. B. Hanan (1998), Chaotic topography, mantle flow and mantle migration in the Australian-Antarctic discordance, *Nature*, *394*, 637–644, doi:10.1038/29226.

Christie, D. M., D. G. Pyle, R. B. Pedersen, and D. J. Miller (2004), Leg 187 synthesis: Evolution of the Australian Antarctic Discordance, the Australian Antarctic Depth Anomaly, and the Indian/Pacific mantle isotopic boundary, *Proc. Ocean Drill. Program Sci. Results*, *187*, 1–41.

Cochran, J. R., and M. Talwani (1977), Free-air gravity anomalies in the world's oceans and their relationship to residual elevation, *Geophys. J.*, *50*, 495–552, doi:10.1111/j.1365-246X.1977.tb01334.x.

Crough, S. T. (1983), The correction for sediment loading on the seafloor, *J. Geophys. Res.*, *88*, 6449–6454, doi:10.1029/JB088iB08p06449.

Divins, D. L. (2004), Total sediment thickness of the world's oceans and marginal seas, ETOPO2v2, global gridded 2-minute database, http://www.ngdc.noaa.gov/mgg/global/etopo2.html, Natl. Geophys. Data Cent., NOAA, U.S. Dep. of Commer., Boulder, Colo.

Forsyth, D. W., R. L. Ehrenbard, and S. Chapin (1987), Anomalous upper mantle beneath the Australian-Antarctic discordance, *Earth Planet. Sci. Lett.*, *84*, 471–478, doi:10.1016/0012-821X(87)90011-2.

Géli, L., J. Cochran, T. Lee, J. Francheteau, C. Labails, C. Fouchet, and D. Christie (2007), Thermal regime of the Southeast Indian Ridge between 88°E and 140°E: Remarks on the subsidence of the ridge flanks, *J. Geophys. Res.*, *112*, B10101, doi:10.1029/2006JB004578.

Gradstein, F. M., F. P. Agterberg, J. G. Ogg, S. Hardenbol, P. Vanveen, J. Thierry, and Z. H. Huang (1994), A Mesozoic time scale, *J. Geophys. Res.*, *99*, 24,051–24,074, doi:10.1029/94JB01889.

Gurnis, M., and R. D. Müller (2003), Origin of the Australian Antarctic Discordance from an ancient slab and mantle wedge, in *Evolution and Dynamics of the Australian Plate*, edited R. R. Hillis, and R. D. Müller, *Spec. Publ. Geol. Soc. Aust.*, *22*, 417–429.

Gurnis, M., R. D. Muller, and L. Moresi (1998), Cretaceous vertical motion of Australia and the Australian-Antarctic Discordance, *Science*, *279*, 1499–1504, doi:10.1126/science.279.5356.1499.

Gurnis, M., L. Moresi, and R. D. Müller (2000), Models of mantle convection incorporating plate tectonics: The Australian region since the Cretaceous, in *The History and Dynamics of Global Plate Motions*, *Geophys. Monogr. Ser.*, vol. 121, edited by M. A. Richards, R. Gordon, and R. van der Hilst, pp. 211–238, AGU, Washington, D. C.

Hayes, D. (1976), Nature and implications of asymmetric seafloor spreading—"Different rates for different plates," *Geol. Soc. Am. Bull.*, *87*, 994–1002, doi:10.1130/0016-7606(1976)87<994:NAIOAS>2.0.CO;2.

Hayes, D. E. (1988), Age-depth relationships and depth anomalies in the southeast Indian Ocean and South Atlantic Ocean, *J. Geophys. Res.*, *93*, 2937–2954, doi:10.1029/JB093iB04p02937.

Hayes, D. E., and J. R. Conolly (1972), Morphology of the southeast Indian Ocean, in *Antarctic Oceanology II: The Australian–New Zealand Sector*, *Antarct. Res. Ser.*, vol. 19, edited by D. E. Hayes, pp. 125–146, AGU, Washington, D. C.

Holmes, R. C., M. Tolstoy, J. R. Cochran, and J. S. Floyd (2008), Crustal thickness variations along the Southeast Indian Ridge (100°–116°E) from 2-D body wave tomography, *Geochem. Geophys. Geosyst.*, *9*, Q12020, doi:10.1029/2008GC002152.

Holmes, R. C., M. Tolstoy, A. J. Harding, J. A. Orcutt, and J. Phipps Morgan (2010), Australian Antarctic Discordance as a simple mantle boundary, *Geophys. Res. Lett.*, *37*, L09309, doi:10.1029/2010GL042621.

Kempton, P. D., J. A. Pearce, T. L. Barry, J. G. Fitton, C. Langmuir, and D. M. Christie (2002), Sr-Nd-Pb-Hf isotope results from ODP Leg 187: Evidence for mantle dynamics of the Australian-Antarctic Discordance and origin of the Indian MORB, *Geochem. Geophys. Geosyst.*, *3*(12), 1074, doi:10.1029/2002GC000320.

Klein, E. M., and C. H. Langmuir (1987), Global correlations of ocean ridge basalt chemistry with axial depth and crustal thickness, *J. Geophys. Res.*, *92*, 8089–8115, doi:10.1029/JB092iB08p08089.

Klein, E. M., C. H. Langmuir, A. Zindler, H. Staudigel, and B. Hamelin (1988), Isotope evidence of a mantle convection boundary at the Australian-Antarctic Discordance, *Nature*, *333*, 623–629, doi:10.1038/333623a0.

Kuo, B. Y. (1993), Thermal anomalies beneath the Australian-Antarctic discordance, *Earth Planet. Sci. Lett.*, *119*, 349–364, doi:10.1016/0012-821X(93)90143-W.

Kuo, B. Y., W. J. P. Morgan, and D. W. Forsyth (1984), Asymmetry in topography of the crestal mountains near a ridge-transform intersection, *Eos, Trans. AGU*, *65*(16), 274.

Kuo, B. Y., C. H. Chen, and Y. S. Zhang (1996), A fast velocity anomaly to the west of the Australian-Antarctic discordance, *Geophys. Res. Lett.*, *23*, 2239–2242, doi:10.1029/96GL02144.

Lin, S., L. Chiao, and B. Kuo (2002), Dynamic interaction of cold anomalies with the mid-ocean ridge flow field and its implications for the Australian-Antarctic Discordance, *Earth Planet. Sci. Lett.*, *203*, 925–935, doi:10.1016/S0012-821X(02)00948-2.

Louden, K. E., B. E. Tucholke, and G. N. Oakey (2004), Regional anomalies of sediment thickness, basement depth and isostatic crustal thickness in the North Atlantic Ocean, *Earth Planet. Sci. Lett.*, *224*, 193–211, doi:10.1016/j.epsl.2004.05.002.

Malinverno, A. (1991), Inverse square-root dependence of mid-ocean-ridge flank roughness on spreading rate, *Nature*, *352*, 58–60, doi:10.1038/352058a0.

Malinverno, A., and R. Pockalny (1990), Abyssal hill topography as an indicator of episodicity in crustal accretion and deformation, *Earth Planet. Sci. Lett.*, *99*, 154–169, doi:10.1016/0012-821X(90)90079-D.

Marks, K. M., P. R. Vogt, and S. A. Hall (1990), Residual depth anomalies and the origin of the Australian-Antarctic Discordance Zone, *J. Geophys. Res.*, *95*, 17,325–17,337, doi:10.1029/JB095iB11p17325.

Marks, K. M., J. M. Stock, and K. J. Quinn (1999), Evolution of the Australian-Antarctic discordance since Miocene time, *J. Geophys. Res.*, *104*, 4967–4981, doi:10.1029/1998JB900075.

Masters, G., G. Laske, H. Bolton, and A. Dziewonski (2000), The relative behavior of shear velocity, bulk sound speed, and compressional velocity in the mantle: Implications for chemical and thermal structure, in *Earth's Deep Interior: Mineral Physics and Tomography From the Atomic to the Global Scale*, *Geophys. Monogr. Ser.*, vol. 117, edited by S. Karato et al., pp. 63–87, AGU, Washington, D. C.

Mégnin, C., and B. Romanowicz (2000), The three-dimensional shear velocity structure of the mantle from the inversion of body, surface and higher-mode waveforms, *Geophys. J. Int.*, *143*, 709–728, doi:10.1046/j.1365-246X.2000.00298.x.

Meyzen, C. M., M. J. Toplis, E. Humler, J. N. Ludden, and C. Mevel (2003), A discontinuity in mantle composition beneath the southwest Indian ridge, *Nature*, *421*, 731–733, doi:10.1038/nature01424.

Meyzen, C. M., J. N. Ludden, E. Humler, B. Luais, M. J. Toplis, C. Mével, and M. Storey (2005), New insights into the origin and distribution of the DUPAL isotope anomaly in the Indian Ocean mantle from MORB of the Southwest Indian Ridge, *Geochem. Geophys. Geosyst.*, *6*, Q11K11, doi:10.1029/2005GC000979.

Montési, L. G. J., and M. D. Behn (2007), Mantle flow and melting underneath oblique and ultraslow mid-ocean ridges, *Geophys. Res. Lett.*, *34*, L24307, doi:10.1029/2007GL031067.

Muller, M. R., T. A. Minshull, and R. S. White (1999), Segmentation and melt supply at the Southwest Indian Ridge, *Geology*, *27*, 867–870, doi:10.1130/0091-7613(1999)027<0867:SAMSAT>2.3.CO;2.

Müller, R. D., M. Sdrolias, C. Gaina, and W. R. Roest (2008), Age, spreading rates, and spreading asymmetry of the world's ocean crust, *Geochem. Geophys. Geosyst.*, *9*, Q04006, doi:10.1029/2007GC001743.

National Geophysical Data Center (2006), 2-minute gridded global relief data, ETOPO2v2, http://www.ngdc.noaa.gov/mgg/fliers/06mgg01.html, NOAA, U.S. Dep. of Commer., Boulder, Colo.

O'Brien, P. E., and H. M. J. Stagg (2007), Tectonic elements of the continental margin of East Antarctica, 38–164°E, in *Antarctica: A Keystone in a Changing World—Online Proceedings of the 10th International Symposium on Antarctic Earth Sciences*, edited by A. K. Cooper, *U.S. Geol. Surv. Open File Rep., 2007–1047*.

Pribac, F. (1991), Superswells due to mantle convection, Ph.D. thesis, Aust. Natl. Univ., Canberra, ACT.

Pyle, D. G., D. M. Christie, J. J. Mahoney, and R. A. Duncan (1995), Geochemistry and geochronology of ancient Southeast Indian and Southwest Pacific seafloor, *J. Geophys. Res.*, *100*, 22,261–22,282, doi:10.1029/95JB01424.

Ritsema, J., and H. J. Van Heijst (2000), Seismic imaging of structural heterogeneity in Earth's mantle: Evidence for large-scale mantle flow, *Sci. Prog.*, *83*, 243–259.

Ritzwoller, M. H., N. M. Shapiro, and G. M. Leahy (2003), A resolved mantle anomaly as the cause of the Australian-Antarctic Discordance, *J. Geophys. Res.*, *108*(B12), 2559, doi:10.1029/2003JB002522.

Sandwell, D., and W. H. F. Smith (2005), Retracking ERS-1 altimeter waveforms for optimal gravity field recovery, *Geophys. J. Int.*, *163*, 79–89, doi:10.1111/j.1365-246X.2005.02724.x.

Sayers, J., P. A. Symonds, N. G. Direen, and G. Bernadel (2001), Nature of the continent-ocean transition on the non-volcanic rifted margin in the central Great Australian Bight, in *Non-volcanic Rifting of Continental Margins: A Comparison of Evidence From Land and Sea*, edited by R. C. L. Wilson et al., *Geol. Soc. London Spec. Publ.*, *187*, 51–76.

Small, C., and D. T. Sandwell (1989), An abrupt change in ridge-axis gravity with spreading rate, *J. Geophys. Res.*, *94*, 17,383–17,392, doi:10.1029/JB094iB12p17383.

Small, C., J. R. Cochran, J. C. Sempere, and D. Christie (1999), The structure and segmentation of the Southeast Indian Ridge, *Mar. Geol.*, *161*(1), 1–12.

Smith, W. H. F. (1998), Seafloor tectonic fabric from satellite altimetry, *Annu. Rev. Earth Planet. Sci.*, *26*, 697–747, doi:10.1146/annurev.earth.26.1.697.

Smith, W. H. F., and D. T. Sandwell (1997), Global sea floor topography from satellite altimetry and ship depth soundings, *Science*, *277*, 1956–1962, doi:10.1126/science.277.5334.1956.

Stagg, H. M. J., and J. B. Colwell (2003), The deep-water East Antarctic continental margin, from 38–152°E: Overview of a new integrated geophysical data set, in *Terra Nostra—Abstracts 9th International Symposium on Antarctic Earth Sciences*, edited by D. K. Fütterer, pp. 307–308, Alfred Wegener Stiftung, Berlin.

Stagg, H. M. J., J. B. Colwell, N. G. Direen, P. E. O'Brien, B. J. Brown, G. Bernardel, I. Borissova, L. Carson, and D. B. Close (2005), Geological framework of the continental margin in the region of the Australian Antarctic Territory, *Record 2004/25*, Geosci. Aust., Canberra, ACT.

Sykes, T. J. S. (1996), A correction for sediment load upon the ocean floor: Uniform versus varying sediment density estimations—Implications for isostatic correction, *Mar. Geol.*, *133*, 35–49, doi:10.1016/0025-3227(96)00016-3.

Tolstoy, M., A. J. Harding, J. A. Orcutt, and M. J. Phipps (1995), Crustal thickness at the Australian Antarctic Discordance and neighboring South East Indian Ridge, *Eos Trans. AGU*, *76*(46), 570.

Turcotte, D. L., and E. R. Oxburgh (1967), Finite amplitude convection cells and continental drift, *J. Fluid Mech.*, *28*, 29–42, doi:10.1017/S0022112067001880.

Veevers, J. J. (1982), Australian-Antarctic depression from the mid-ocean ridge to adjacent continents, *Nature*, *295*, 315–317, doi:10.1038/295315a0.

Weissel, J. K., and D. E. Hayes (1971), Asymmetric seafloor spreading south of Australia, *Nature*, *231*, 518–522, doi:10.1038/231518a0.

Weissel, J. K., and D. E. Hayes (1974), The Australian-Antarctic Discordance: New results and implications, *J. Geophys. Res.*, *79*, 2579–2587, doi:10.1029/JB079i017p02579.

Wessel, P., and W. H. F. Smith (1991), Free software helps map and display data, *Eos Trans. AGU*, *72*, 441–446, doi:10.1029/90EO00319.

West, B. P., W. S. D. Wilcock, J. C. Sempere, and L. Géli (1997), Three-dimensional structure of asthenospheric flow beneath the Southeast Indian Ridge, *J. Geophys. Res.*, *102*, 7783–7802, doi:10.1029/96JB03895.

West, B., J. Lin, and D. Christie (1999), Forces driving ridge propagation, *J. Geophys. Res.*, *104*, 22,845–22,858, doi:10.1029/1999JB900154.

White, R. S., D. McKenzie, and R. K. O'Nions (1992), Oceanic crustal thickness from seismic measurements and rare earth element inversion, *J. Geophys. Res.*, *97*, 19,683–19,715, doi:10.1029/92JB01749.

Whittaker, J. M., R. D. Müller, G. Leitchenkov, H. Stagg, M. Sdrolias, C. Gaina, and A. Goncharov (2007), Major Australian-Antarctic plate reorganisation at Hawaiian-Emperor bend time, *Science*, *318*, 83–86, doi:10.1126/science.1143769.

Whittaker, J. M., R. D. Müller, W. R. Roest, P. Wessel, and W. H. F. Smith (2008), How supercontinents and supero-ceans affect seafloor roughness, *Nature*, *456*, 938–941, doi:10.1038/nature07573.

Zhang, Y. S., and T. Tanimoto (1993), High-resolution global upper mantle structure and plate tectonics, *J. Geophys. Res.*, *98*, 9793–9823, doi:10.1029/93JB00148.